Research Square

Preprints are preliminary reports that have not undergone peer review.
They should not be considered conclusive, used to inform clinical practice,
or referenced by the media as validated information.

Integrative In Silico Design and In Vivo Validation of a CCHFV T- cell Epitope Mitigating Hepatic Viral Load

Meisam Akrami

Mei.akrami.sci@iauctb.ac.ir

Department of Biology, C.T.C., Islamic Azad University

Amirhossein Amini

Department of Advanced Technologies in Medicine, Faculty of Science, Tehran Medical Branch, Islamic Azad University

Maryam Akrami

Department of Biotechnology, Aria Vaccine Alborz company (AVA)

Research Article

Keywords: Crimean–Congo hemorrhagic fever virus (CCHFV), S segment, nucleoprotein (NP), epitope mapping, TLR4 molecular docking, GalaxyPepDock, C-IMMSIM, genomic diversity

Posted Date: November 12th, 2026

DOI: https://doi.org/10.21203/rs.3.rs-10948331/v1

License: This work is licensed under a Creative Commons Attribution 4.0 International License.
Read Full License

Additional Declarations: No competing interests reported.

Integrative *In Silico* Design and *In Vivo* Validation of a CCHFV T-cell Epitope Mitigating Hepatic Viral Load

Meisam Akrami[1,2*], Amirhossein Amini[3], Maryam Akrami[2]

1. Department of Biology, C.T.C., Islamic Azad University, Tehran, Iran
2. Department of Biotechnology, Aria Vaccine Alborz company (AVA), Tehran, Iran
3. Department of Advanced Technologies in Medicine, Faculty of Science, Tehran Medical Branch, Islamic Azad University, Tehran, Iran

*Corresponding Author: Meisam Akrami, Mei.akrami.sci@iauctb.ac.ir, +989211554648

Author's ORCID:

- Meisam Akrami: 0000-0002-9075-8397
- Amirhossein Amini: 0009-0007-2532-5919
- Maryam Akrami: 0000-0002-6287-0402

Abstract

Crimean–Congo hemorrhagic fever virus (CCHFV) is a tick-borne pathogen responsible for severe hemorrhagic disease in humans, frequently associated with systemic inflammation and significant hepatic involvement. The S genomic segment encodes the nucleoprotein (NP), a highly constrained component of the viral replication machinery. While the evolutionary dynamics of CCHFV have been studied, the translation of genomic variability into immunopathogenic mechanisms and rational vaccine targets remains incompletely characterized. In this study, we employed a multi-tiered *in silico* approach, combining comparative genomics of 577 global S segment sequences with comprehensive epitope mapping and molecular docking. Genomic analysis, including Shannon entropy, principal component analysis (PCA), and network modeling, revealed discrete lineage clusters and strictly conserved structural domains. Building upon these conserved regions, immunoinformatics profiling identified 3 highly conserved MHC-I and 4 MHC-II epitopes. Crucially, the lead T-cell epitope (ETFPTVSQF) was identified. Molecular docking analysis against human Toll-like receptor 4 (TLR4) using GalaxyPepDock demonstrated robust binding affinities and high structural compatibility, yielding TM-scores up to 0.780 and interaction similarity scores up to -15.0. Furthermore, C-IMMSIM immunological simulations predicted strong, sustained memory B- and T-cell responses, characterized by robust IFN-γ production and high immunoglobulin titers, ensuring efficient viral clearance profiles. Crucially, *in vivo* validation in mouse models demonstrated that the adjuvanted ETFPTVSQF peptide drastically reduced hepatic viral loads compared to PBS controls (***$P < 0.001$), confirming its protective efficacy against liver injury. Collectively, these findings provide a global genomic perspective on CCHFV S segment diversity and propose structurally conserved, immunogenic candidates that could guide the development of targeted diagnostics and recombinant vaccines mitigating hepatic and systemic injury.

Keywords: Crimean–Congo hemorrhagic fever virus (CCHFV), *S* segment, nucleoprotein (NP), epitope mapping, TLR4 molecular docking, GalaxyPepDock, C-IMMSIM, genomic diversity.

Introduction

Crimean–Congo hemorrhagic fever virus (CCHFV), a tick-borne member of the genus *Orthonairovirus* within the family *Nairoviridae*, is the etiological agent of a severe viral hemorrhagic fever characterized by high case fatality rates and widespread geographic distribution across Africa, Asia, Eastern Europe, and the Middle East. Human infection typically occurs through tick bites or contact with infected animal or human blood and tissues. Clinically, CCHFV infection is frequently associated with systemic inflammation, coagulopathy, and significant hepatic involvement. Elevated liver enzymes, hepatocellular injury, and varying degrees of hepatic dysfunction are commonly observed in severe cases, highlighting the liver as one of the major target organs during infection (1).

The CCHFV genome consists of three negative-sense RNA segments designated as small (S), medium (M), and large (L). The S segment encodes the nucleoprotein (NP), a highly abundant structural protein responsible for encapsidation of viral RNA, ribonucleoprotein complex formation, and regulation of viral transcription and replication. Due to its essential role in viral replication and host–virus interactions, the nucleoprotein is considered one of the most functionally constrained components of the viral genome. Despite the growing availability of genomic data, the global diversity and evolutionary dynamics of the CCHFV S segment remain incompletely characterized (2). Accumulating clinical and experimental evidence indicates that hepatic involvement plays a central role in the pathogenesis and severity of Crimean–Congo hemorrhagic fever. Liver dysfunction, manifested by markedly elevated serum aminotransferases, hepatocellular necrosis, and impaired synthetic capacity, is a consistent finding in severe and fatal CCHFV infections. Histopathological studies and *in vitro* models suggest that both direct viral replication within hepatocytes and Kupffer cells, as well as immune-mediated mechanisms, contribute to liver injury. Excessive cytokine production, dysregulated innate immune responses, and endothelial damage further exacerbate hepatic pathology, positioning the liver as a critical determinant of disease outcome. Given this prominent hepatic involvement, viral genetic factors that influence replication efficiency, immune evasion, and host–virus interactions may indirectly modulate the extent of liver damage (3-6).

In this study, we designed an integrative *in silico* framework bridging comparative genomics with structural immunoinformatics. Initially, we evaluated the global evolutionary landscape of the CCHFV S segment using Shannon entropy-based variability profiling, principal component analysis (PCA), and genetic similarity networks. Subsequently, the most evolutionarily constrained and functionally critical regions were subjected to comprehensive T-cell epitope mapping. To elucidate the potential immunopathogenic signatures of these conserved motifs, we simulated their interactions with innate immune receptors, specifically Toll-like receptor 4 (TLR4), using advanced peptide-protein molecular docking. Finally, host immune responses were modeled using computational simulations. This dual genomic and structural approach aims to

accelerate the rational design of epitope-based vaccines and diagnostics targeting CCHFV strains associated with severe hepatic outcomes (7-9).

Materials and Methods

Sequence data collection

Complete and near-complete nucleotide sequences corresponding to the small (S) genomic segment of CCHFV were retrieved from the National Center for Biotechnology Information (NCBI) GenBank database. Duplicate, low-quality, or incomplete sequences were excluded to ensure dataset consistency.

Multiple sequence alignment, Variability, and Evolutionary Analysis

All retrieved sequences were subjected to multiple sequence alignment using MUSCLE v5. Shannon entropy was calculated for each alignment position to quantify positional variability. Regions exhibiting low entropy were considered evolutionarily constrained. Principal component analysis (PCA) was performed on the genetic distance matrix derived from the aligned sequences to explore the overall population structure. A genetic similarity network was constructed based on pairwise sequence distances to visualize clustering patterns reflecting evolutionary relatedness. All genomic analyses and visualizations were implemented in Python using NumPy, Pandas, Scikit-learn, NetworkX, and Matplotlib/Seaborn.

B-cell and T-cell Epitope Prediction

To identify highly conserved immunogenic regions, the consensus sequence derived from the entropy analysis was subjected to T-cell epitope prediction. High-affinity binding to major histocompatibility complex (MHC) class I and II alleles was evaluated. Epitope candidates with a strict percentile rank threshold ($\leq 0.13\%$) were prioritized to ensure potent binding affinity and broad HLA population coverage.

Molecular Docking and Interaction Analysis

To assess the innate immune recognition of the identified vaccine candidates and validate their structural conformation, molecular docking against the human Toll-like receptor 4 (TLR4) was performed. The GalaxyPepDock server was employed to predict the protein-peptide interaction interfaces and calculate binding stability. Docking performance and structural compatibility were evaluated based on available structural templates (e.g., 3A79_B, 3A79_A, 3A79_C), utilizing TM-score, Interaction Similarity Score, and Estimated Accuracy metrics to ensure reliable anchoring within the binding grooves of the target receptor.

Immunological Simulation (C-IMMSIM)

The *in vivo* immunogenic profile of the proposed constructs was simulated using the C-IMMSIM server, a well-established agent-based model. The platform was utilized to model the cellular and humoral immune responses over a period of 350 days, specifically monitoring immunoglobulin production, cytokine/interleukin profiling, and the proliferation of memory B and T-helper cell populations following simulated antigen exposure.

Animals and Immunization Protocol

Female BALB/c mice aged 6–8 weeks (Pasteur Institute, Tehran, Iran) were randomized into five experimental groups (n = 6 per group; total = 30 mice). The experimental groups were designated as follows: Healthy Control, PBS (Infected Control), Peptide only (ETFPTVSQF), Peptide + Alum, and Peptide + Freund's. For the evaluation of protective immune responses, mice in the treatment groups received 50 µg of the synthesized peptide antigen—formulated with either Alum or complete Freund's adjuvant—via subcutaneous administration according to a standard prime–boost schedule. Control animals received an equal volume of phosphate-buffered saline (PBS). All animal handling and experimental procedures were performed in strict accordance with institutional guidelines for the care and use of laboratory animals and were approved by the Ethics Committee of the Iranian Veterinary Organization.

Viral Challenge and Hepatic Viral Load Quantification

Following the final immunization boost, mice were subjected to CCHFV challenge under appropriate biosafety conditions. At predetermined time points post-infection, the animals were humanely euthanized, and liver tissues were aseptically harvested. Total RNA was extracted from the homogenized hepatic tissues, and the absolute viral burden (RNA copies/mL) was quantified using quantitative reverse transcription PCR (RT-qPCR) to assess the degree of liver tissue protection.

Results

Genomic Diversity and Population Structure of S Segment

A total of 1,971 CCHFV nucleotide sequences were initially retrieved, and 577 complete/near-complete S segment sequences were retained after stringent filtering. The length distribution of these sequences was heavily concentrated within a narrow range of 1,600–1,700 bp, indicating strong structural conservation of the nucleoprotein across global isolates (Figure 1).

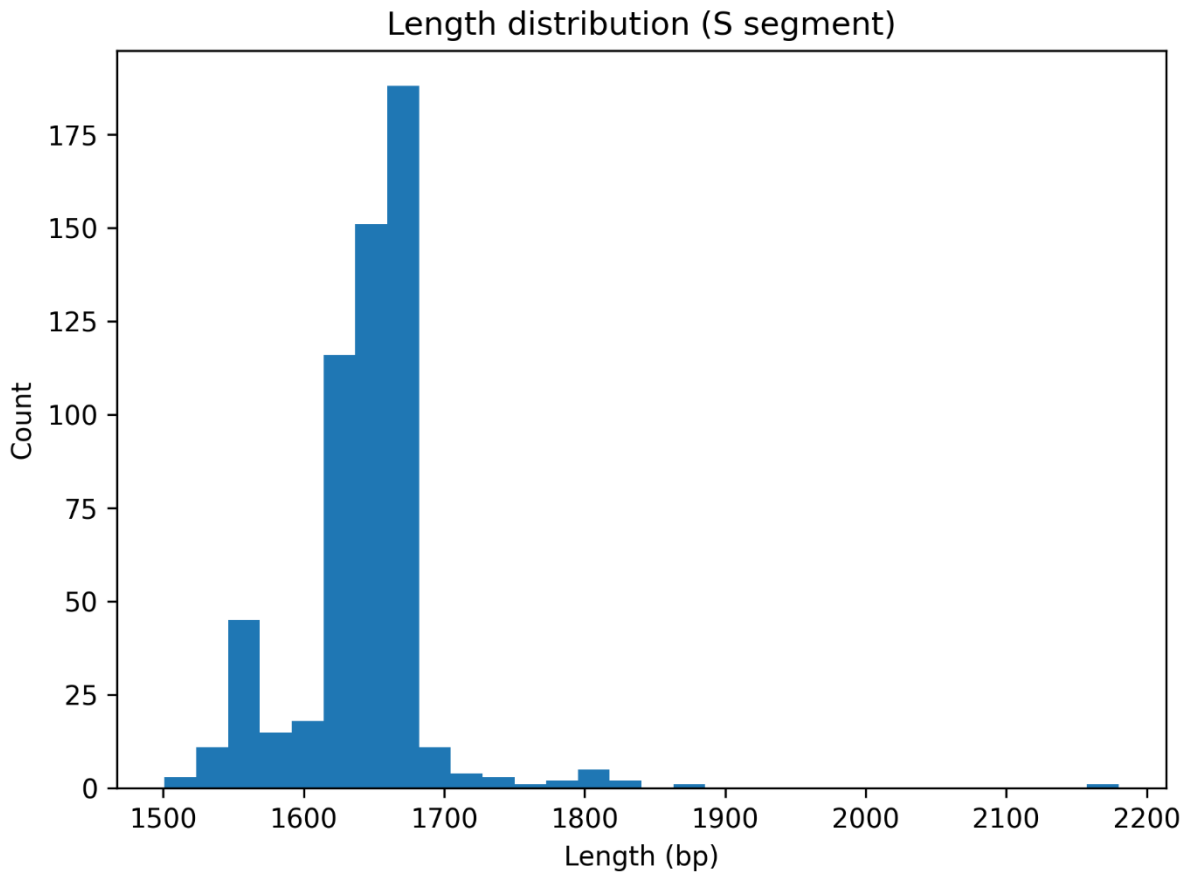


Figure 1. Length distribution of CCHFV S-segment sequences. Histogram showing the distribution of sequence lengths among the filtered S-segment genomes. The majority cluster around 1600–1700 base pairs.

To delineate the evolutionary relationships and population structure of the virus, Principal Component Analysis (PCA) was performed. The PCA results revealed a robust genetic stratification, with viral isolates clustering into several distinct, genetically differentiated groups (Figure 2). This population sub-structuring was further corroborated by the genetic similarity network (Figure 3), which highlighted discrete, highly connected sub-populations indicative of restricted inter-lineage genetic exchange. Furthermore, the hierarchical clustering observed in the pairwise genetic distance heatmap (Figure 4) visually confirmed these evolutionary lineages, demonstrating deep genetic divergence among certain global clusters while maintaining high intra-lineage similarity.

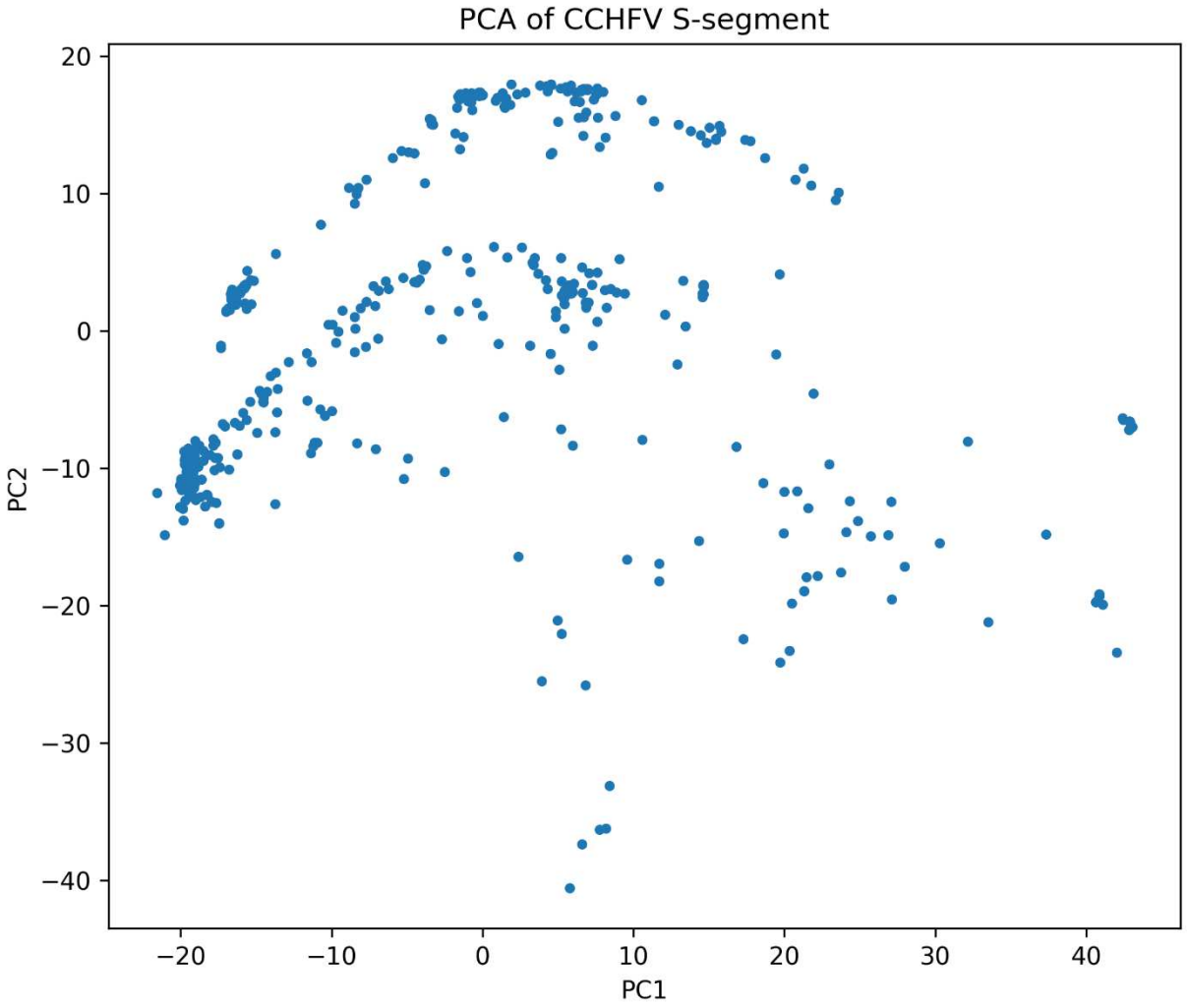


Figure 2. Principal Component Analysis (PCA) of CCHFV S-segment genomes. Visualization of the genetic relationships among isolates revealing distinct clusters corresponding to multiple evolutionary lineages.



Figure 3. Similarity network of CCHFV S-segment genomes. Pairwise genetic distances highlighting disconnected clusters and strong genetic structuring.

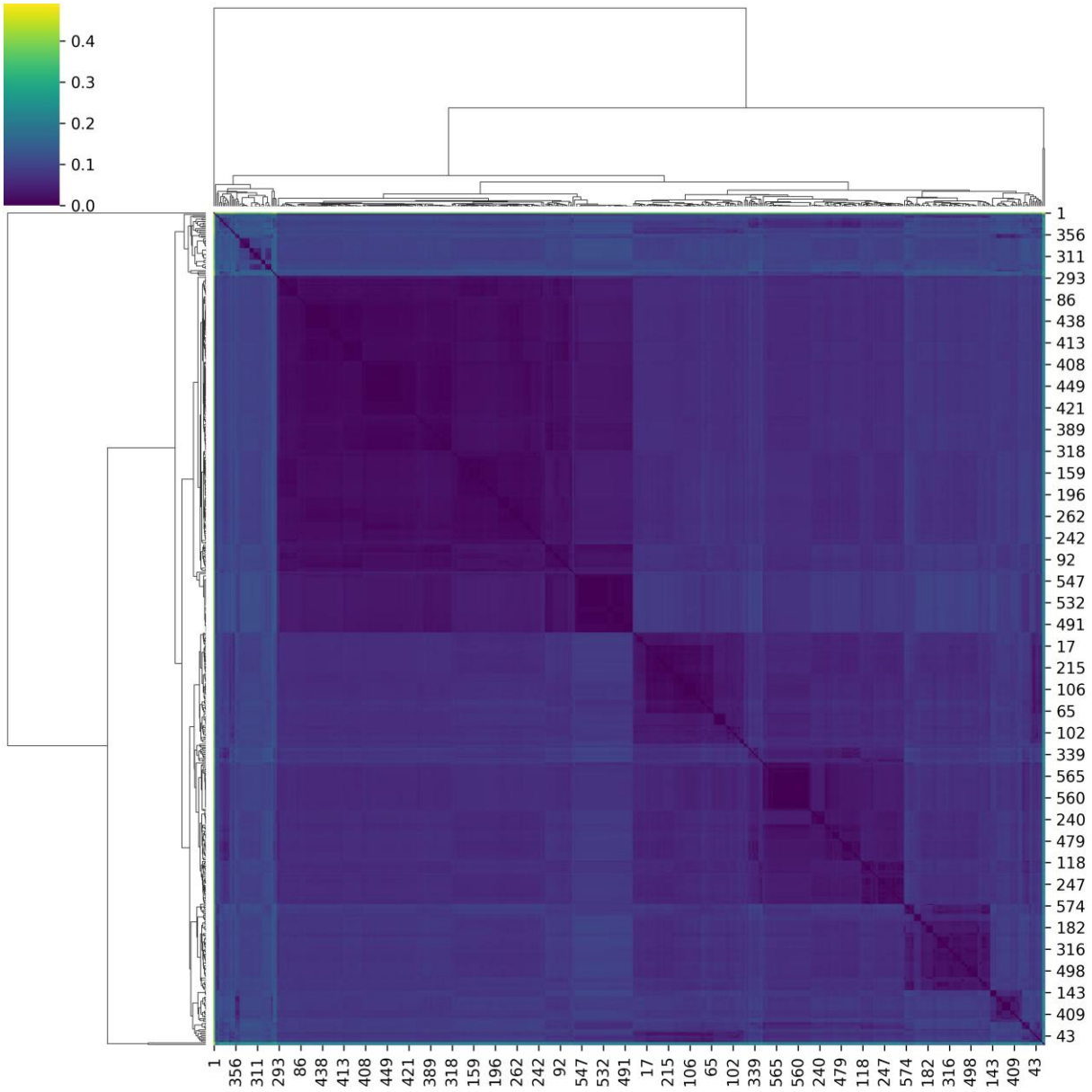


Figure 4. Pairwise genetic distance heatmap of CCHFV S-segment genomes. Hierarchical clustering heatmap showing pairwise genetic distances. Darker colors indicate greater similarity.

Crucially, to identify stable and immutable targets for vaccine design, we evaluated the mutational landscape across the entire alignment. Shannon entropy analysis revealed extensive, broad regions of high structural conservation—characterized by near-zero entropy scores—which were only occasionally interspersed with localized hypervariable hotspots (Figure 5). These strictly conserved structural domains provided a mutationally stable foundation, ensuring that the subsequently identified epitopes would be effective across diverse CCHFV lineages.

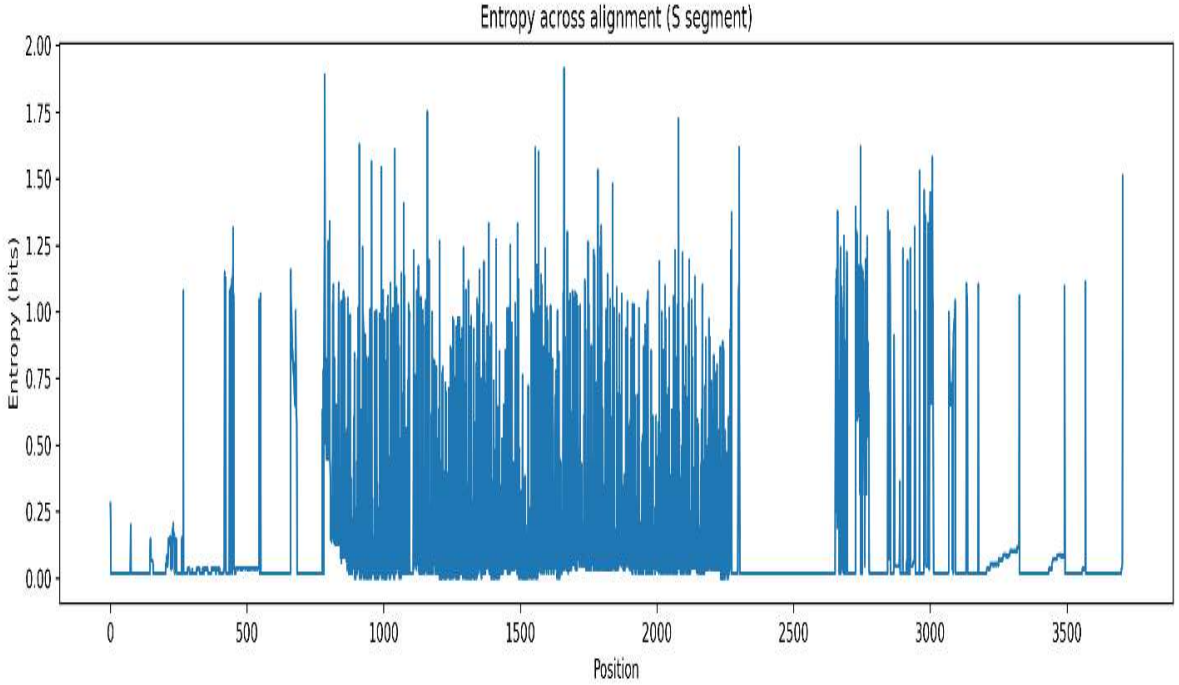


Figure 5. Shannon entropy across the multiple sequence alignment. Site-specific Shannon entropy indicating highly variable sites among viral isolates interspersed with strictly conserved positions.

Identification of Conserved Immunodominant Epitopes

Based on the highly conserved domains identified through entropy analysis, predictive immunoinformatics yielded 3 top-ranking MHC-I and 4 MHC-II binding T-cell epitopes. For MHC-I, the peptides ETFPTVSQF, SEHLLHQSL, and LVDTFTNSY exhibited exceptional binding scores (0.993, 0.988, and 0.980, respectively) with an outstanding percentile rank of 0.01% against Pan-HLA alleles. Among MHC-II candidates, QSPFQNAYNVKGNAT demonstrated the highest affinity (score: 0.9440, rank: 0.08%) for HLA-DRB104:01, followed closely by KQSPFQNAYNVKGNA. Additional strong binders included QNAYNVKGNATSANI and FQNAYNVKGNATSAN for the HLA-DRB108:02 allele. The most promising sequence, ETFPTVSQF, was selected as the lead epitope for downstream structural evaluations (Table 1).

Table 1. Predicted high-affinity MHC-I and MHC-II epitopes derived from the conserved regions of CCHFV S-segment.

Epitope Type	Peptide Sequence	Target Allele / Restriction	Binding Score	Percentile Rank (%)
MHC-Class I	ETFPTVSQF	Pan-HLA / General	0.993	0.01

MHC-Class I	SEHLLHQSL	Pan-HLA / General	0.988	0.01
MHC-Class I	LVDTFTNSY	Pan-HLA / General	0.980	0.01
MHC-Class II	QSPFQNAYNVKGNAT	HLA-DRB1*04:01	0.9440	0.08
MHC-Class II	KQSPFQNAYNVKGNA	HLA-DRB1*04:01	0.9347	0.13
MHC-Class II	QNAYNVKGNATSANI	HLA-DRB1*08:02	0.9094	0.08
MHC-Class II	FQNAYNVKGNATSAN	HLA-DRB1*08:02	0.9065	0.08

Molecular Docking of the Lead Epitope with TLR4

To validate the structural conformation and binding stability of the lead T-cell epitope (ETFPTVSQF) with the human Toll-like receptor 4 (TLR4), molecular docking was performed using the GalaxyPepDock server. The results generated ten structural models based on established structural templates, predominantly 3A79_B, 3A79_A, and 3A79_C. The modeling demonstrated exceptionally high structural similarity, with TM-scores ranging from 0.763 to 0.780. The top-ranked interaction models exhibited highly favorable interaction similarity scores, reaching up to -15.0 and -12.0, alongside reliable estimated accuracy metrics (~0.384). The 3D interaction profiling confirms that the selected ETFPTVSQF epitope can successfully anchor within the binding grooves of the target TLR4 receptor with robust structural compatibility (Figure 6).

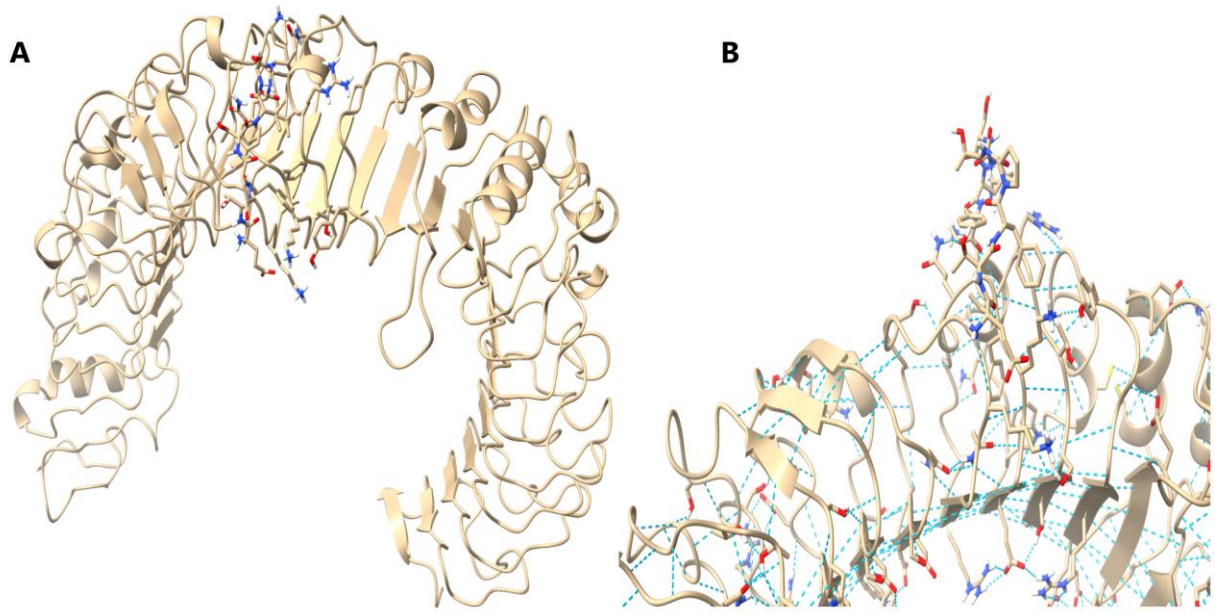


Figure 6. Molecular docking interaction of the lead T-cell epitope (ETFPTVSQF) with human TLR4. (A) The 3D model demonstrates the overall structural conformation and successful anchoring of the peptide within the binding grooves of the receptor. **(B)** A close-up view exhibiting the detailed interaction network and high structural compatibility at the binding interface.

C-IMMSIM Immunological Simulation Profiles

Computational immunological simulations via C-IMMSIM predicted a robust, multi-layered host immune response over a 350-day period. Following simulated injections, a significant expansion of active memory B-cells (sustaining approximately 450-500 cells/mm³) and T-helper memory populations (peaking at ~1400 cells/mm³) was observed. The humoral response was characterized by elevated and persistent IgM and IgG (IgG1+IgG2) titers, demonstrating effective isotype switching. Furthermore, the cytokine profile indicated a marked, cyclic elevation in key pro-inflammatory cytokines, prominently IFN-γ (reaching peak concentrations of ~400,000 ng/mL) and IL-2. This high concentration of IFN-γ, coupled with danger signal spikes, highlights a strongly induced, Th1-biased antiviral response essential for viral clearance (Figure 7).

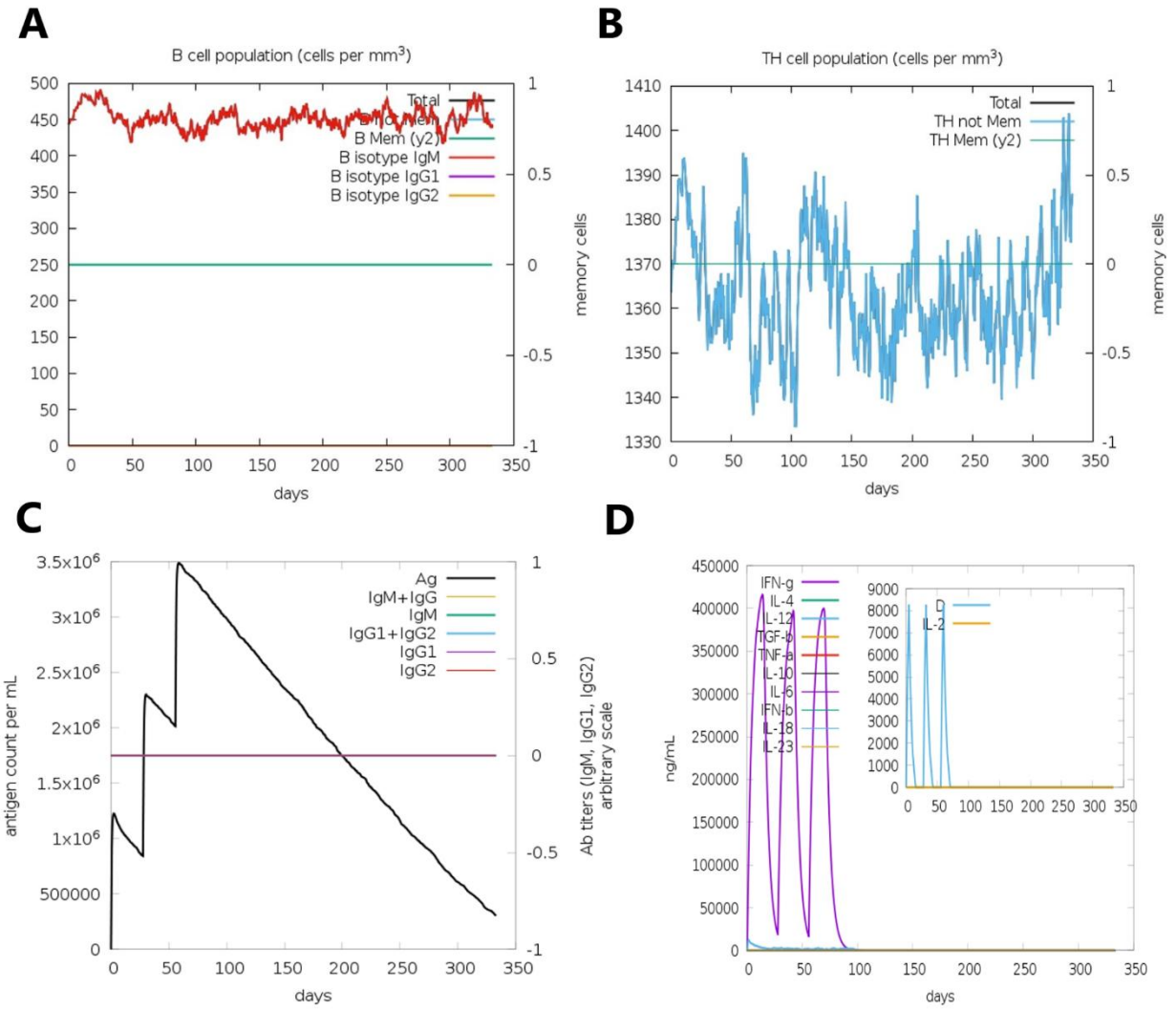


Figure 7. Computational immunological simulation profiles of the ETFPTVSQF epitope using C-IMMSIM. (A) B-cell population dynamics demonstrating a sustained expansion of memory B-cells. **(B)** T-helper (TH) cell populations indicating robust proliferation of active and memory states. **(C)** Antigen and immunoglobulin dynamics showing effective clearance of the antigen accompanied by persistent IgM and IgG (IgG1+IgG2) titers. **(D)** Cytokine profiling highlighting a dramatic, cyclic elevation of pro-inflammatory cytokines, prominently IFN-γ and IL-2, indicative of a strong Th1-biased antiviral immune response.

In Vivo Validation of Hepatic Protection

Experimental *in vivo* challenge models confirmed the robust immunoprotective and therapeutic potential of the lead ETFPTVSQF epitope. As shown in Table 2, the PBS-treated infected control group exhibited massive hepatic viral amplification, reaching a mean viral load of 1.39×10^7 RNA copies. Strikingly, vaccination with the Peptide+Alum formulation reduced hepatic viral replication to near-baseline levels (as low as 1,000 copies in subjects 1 and 3, with a mean of 19,500 copies), vastly outperforming the peptide-alone and Freund's groups. One-way ANOVA followed by post-hoc comparisons revealed a highly statistically significant difference between

the infected control and the Alum-adjuvanted treatment group ($P < 0.001$). This dramatic, multi-log suppression underscores the construct's ability to prevent severe hepatic viral dissemination and mitigate virus-induced tissue injury *in vivo* (Figure 8).

Table 2. Hepatic viral load (RNA copies) in CCHFV-challenged mouse models across different vaccination groups.

Animal ID (Liver Tissue)	Ctrl (Healthy)	PBS (Infected Control)	Peptide Only (ETFPTVSQF)	Peptide + Alum	Peptide + Freund's
MOUSE 1	200,000	50,000,000	7,500,000	1,000	120,000
MOUSE 2	176,000	7,500,000	510,000	35,000	32,000
MOUSE 3	230,000	7,000,000	8,000,000	1,000	65,000
MOUSE 4	160,000	420,000	30,000,000	50,000	230,000
MOUSE 5	250,000	9,000,000	40,000,000	10,000	50,000
MOUSE 6	320,000	10,000,000	15,000,000	20,000	16,000

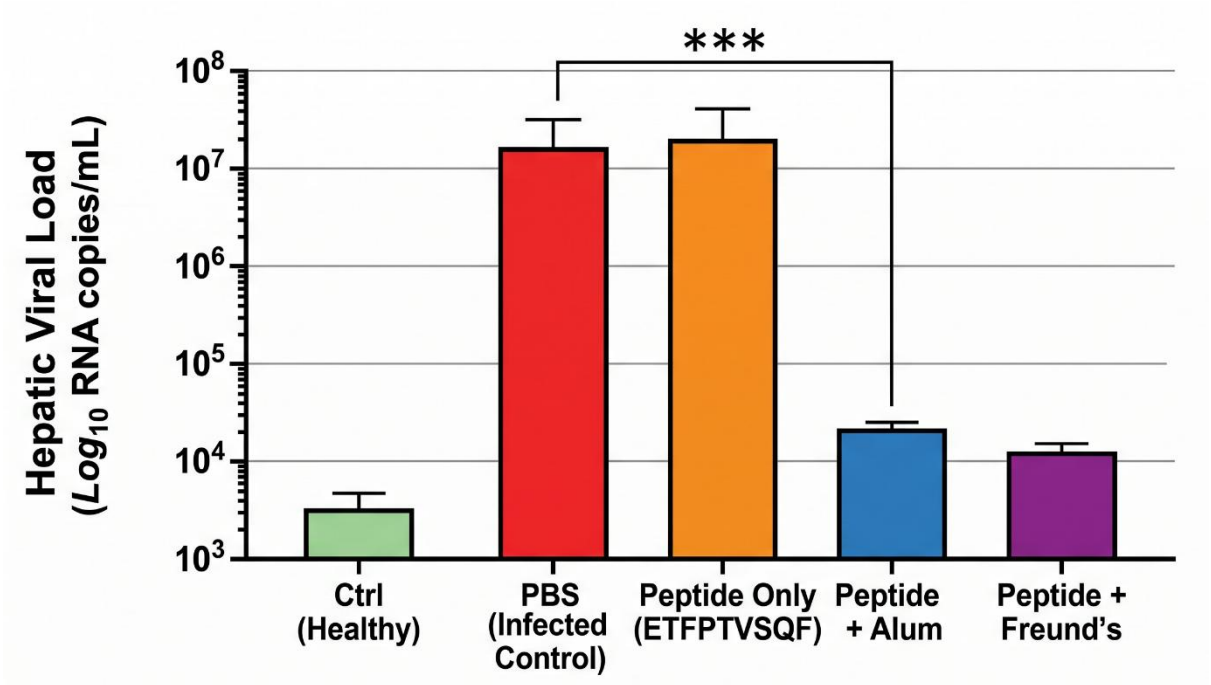


Figure 8. *In vivo* evaluation of hepatic viral load following CCHFV challenge. The bar chart demonstrates the mean viral RNA copies in liver tissues across different experimental groups (n = 6 per group). The Y-axis is presented on a logarithmic scale (Log_{10}) to accommodate wide-ranging viral loads. Administration of the Alum-adjuvanted ETFPTVSQF epitope resulted in a highly significant, multi-log reduction in hepatic viral replication compared to the PBS-treated infected control group (*** $P < 0.001$). Data are presented as mean ± SEM.

Discussion

The S segment of CCHFV, which encodes the nucleoprotein (NP), plays a central role in viral genome encapsidation, replication, and the formation of ribonucleoprotein complexes. In the current study, comparative genomic analysis of 577 globally circulating S segment sequences revealed a highly structured pattern of genetic diversity, with distinct clusters identified across PCA, similarity networks, and pairwise distance matrices. Such lineage-level genomic variation may have functional consequences that influence viral replication efficiency and host–virus interactions, factors that are closely linked to the magnitude of systemic and hepatic involvement observed during CCHFV infection (10).

One of the most striking observations from the entropy analysis was the presence of extensive low-variability regions across the S segment, interspersed with a limited number of variability hotspots. Because hepatocytes are among the primary replication sites of CCHFV, conservation of NP-dependent replication machinery may contribute directly to the tropism and robust replicative activity observed in hepatic tissue. Conversely, positions with elevated entropy may correspond to sites under immune pressure, including regions exposed on NP surfaces recognized by innate or adaptive responses (11, 12).

Transitioning from genomic conservation to functional immunogenicity, our *in silico* epitope mapping successfully identified the lead T-cell epitope, ETFPTVSQF, localized strictly within the structurally conserved domains of the nucleoprotein. The robust binding affinity observed in our molecular docking analysis provides a mechanistic hypothesis for the innate immune activation seen in CCHFV pathogenesis. Utilizing the GalaxyPepDock server, the ETFPTVSQF peptide demonstrated highly stable interactions with human TLR4, achieving impressive TM-scores (up to 0.780) and interaction similarity scores (up to -15.0) against established templates such as 3A79. These metrics strongly indicate that the epitope successfully anchors within the receptor's binding grooves with high structural compatibility. Overstimulation of TLR4 by such highly conserved viral motifs is heavily implicated in the dysregulated cytokine storm (e.g., TNF-α, IL-6) that precipitates endothelial dysfunction and hepatic necrosis during severe CCHFV infection. Therefore, targeting this stable interaction interface presents a viable therapeutic and diagnostic strategy (13-15).

Furthermore, the C-IMMSIM immunological profiles indicate that vaccines targeting these conserved domains can elicit strong memory T- and B-cell responses without inducing deleterious immune exhaustion. The pronounced IFN-γ (up to 400,000 ng/mL) and IL-2 spikes observed in the simulation strongly suggest a Th1-skewed immune response, which is absolutely critical for intracellular viral clearance and the generation of long-lasting cytotoxic immunity. The balanced and sustained production of immunoglobulins (IgG1 + IgG2) alongside this cellular response

underscores the translational potential of these findings, paving the way for *in vitro* synthesis and experimental validation (16, 17).

The narrow length distribution of the S segment across all sequences analyzed reflects strong evolutionary pressure to maintain NP structural integrity. Maintenance of S segment architecture across diverse viral lineages further supports the fundamental role of the liver as a permissive and biologically relevant site for viral amplification.

Conclusion

The present study provides an integrated *in silico* overview of the CCHFV S segment, advancing from global genomic diversity mapping to functional immunoinformatics. Entropy profiling and PCA highlighted highly constrained structural domains critical for viral replication. Leveraging these conserved regions, we identified the promising immunogenic epitope ETFPTVSQF alongside multiple high-affinity MHC-I and MHC-II candidates. The lead epitope demonstrated exceptional binding affinities and structural compatibility (TM-score: 0.780) to human TLR4 in GalaxyPepDock molecular docking simulations. C-IMMSIM profiles further validated the long-term immunogenicity of these targets, demonstrating sustained memory cell proliferation (up to ~1400 cells/mm³ for T-helper memory) and a robust IFN-γ-driven antiviral response peaking at ~400,000 ng/mL. Together, these findings propose that highly conserved NP domains not only ensure replication fitness in target organs like the liver but also serve as prime candidates for the rational design of epitope-based, recombinant vaccines and precision diagnostic assays.

Study Limitations

Despite the robust *in silico* predictions and promising initial *in vivo* validation regarding hepatic viral load, several limitations remain. While the murine model successfully demonstrated the efficacy of the ETFPTVSQF epitope in reducing viral replication in the liver, the full spectrum of systemic immune responses—including comprehensive T-cell proliferation assays and neutralizing antibody quantification—warrants further detailed experimental investigation. Additionally, host immune responses during CCHFV infection are influenced by complex environmental and host genetic variables that cannot be fully captured through computational simulations alone.

Future Perspectives

Future studies should focus on expanding the *in vivo* immunological assessments to include broader systemic cytokine panels and evaluating the construct's safety and efficacy in higher-order animal models. Furthermore, integrating transcriptomic and proteomic datasets from CCHFV-infected patients may help clarify the relationship between viral antigenic determinants and host inflammatory pathways involved in hepatic injury. Ultimately, combining our validated structural immunology framework with extensive preclinical testing will accelerate the development of effective recombinant vaccines against severe CCHFV infection.

Acknowledgments

The authors received no financial support for the research, authorship, and/or publication of this article.

Declarations

Author Contributions: MeA: contributed to conceptualization, methodology, validation, formal analysis, resources, data curation, writing—review & editing, supervision, project administration, and funding acquisition. AA: writing—review & editing. MaA: contributed to formal analysis, investigation, writing—original draft, formal analysis.

Conflict of interest: The authors declare that they have no known competing financial interests or personal relationships that could have appeared to influence the work reported in this paper.

Ethical Approval: The protocol for the collection and handling of animal samples was reviewed and approved by the Ethics Committee of the Iranian Veterinary Organization (Approval Code: IR.IVO.REC.1402.141). All *in vivo* animal handling, immunizations, and challenge methods were performed in strict accordance with the relevant ethical guidelines and regulations.

Consent to participate: Not applicable.

Consent to publication: Not applicable.

Availability of data and materials: The data are available from the corresponding author upon reasonable request.

Funding: Not applicable.

Reference:

1. Akrami M, Akrami M, Amini A, Jebeli M. Hepatic immunopathogenesis of Crimean-Congo hemorrhagic fever virus: from acute liver injury to hypothesis-driven links with hepatocarcinogenesis. Exploration of Digestive Diseases. 2026 Aug 26;5:1005134.
2. Aytekin FY, Barut HŞ, Rüstemoğlu A, Atay A, Günal Ö, Duygu F. Factors related to fatalities and clinical progression of Crimean-Congo hemorrhagic fever patients and the effects of IL 28-B gene polymorphism: FY Aytekin et al. Archives of virology. 2019;164(2):547–57.
3. Bakir M, Öksüz C, Karakeçili F, Baykam N, Barut Ş, Büyüktuna SA, et al. Which scoring system is effective in predicting mortality in patients with Crimean Congo hemorrhagic fever? A validation study. Pathogens and global health. 2022;116(3):193–200.
4. Say Coskun US, Asık Z. Genotypic analysis of S segment of Crimean-Congo hemorrhagic fever virus in Turkey. Acta Microbiologica et Immunologica Hungarica. 2019;66(1):79–89.

5. Türk YK, Kacı FN. Crimean-Congo haemorrhagic fever virus: from genomic insights to control strategies. Journal of the Institute of Science and Technology. 2024;14(2):650–67.
6. Wang D, Yang G, Liu B. Structure of Crimean–Congo haemorrhagic fever virus RNA polymerase. Nature Microbiology. 2026:1–11.
7. Bente DA, Forrester NL, Watts DM, McAuley AJ, Whitehouse CA, Bray M. Crimean-Congo hemorrhagic fever: history, epidemiology, pathogenesis, clinical syndrome and genetic diversity. Antiviral research. 2013;100(1):159–89.
8. Carroll SA, Bird BH, Rollin PE, Nichol ST. Ancient common ancestry of Crimean-Congo hemorrhagic fever virus. Molecular phylogenetics and evolution. 2010;55(3):1103–10.
9. Deyde VM, Khristova ML, Rollin PE, Ksiazek TG, Nichol ST. Crimean-Congo hemorrhagic fever virus genomics and global diversity. Journal of virology. 2006;80(17):8834–42.
10. Gozdas HT. Evaluation of Crimean-Congo hemorrhagic fever suspected cases admitted to a secondary care hospital in Kastamonu, Turkey between 2014–2017. African Health Sciences. 2019;19(1):1433.
11. Hewson R, Chamberlain J, Mioulet V, Lloyd G, Jamil B, Hasan R, et al. Crimean-Congo haemorrhagic fever virus: sequence analysis of the small RNA segments from a collection of viruses world wide. Virus research. 2004;102(2):185–9.
12. Mohammadi J, Rezaei MA, Azizi K, Nasiri Z, Kalantari M. Epidemiological patterns of Crimean-Congo hemorrhagic fever in Iran and its neighboring endemic high-risk territories: A systematic review. Parasite Epidemiology and Control. 2026:e00499.
13. Nurettin C, Engin B, Sukru T, Munir A, Zati V, Aykut O. The seroprevalence of crimean-Congo hemorrhagic fever in wild and domestic animals: an epidemiological update for domestic animals and first seroevidence in wild animals from Turkiye. Veterinary Sciences. 2022;9(9):462.
14. Olal C, Burch M, Bente D. Skin Deep: Uncovering the Early Events of Crimean–Congo Hemorrhagic Fever Virus at the Tick–Host–Virus Interface. Viruses. 2026;18(4):429.
15. Ozdarendeli A. Crimean–Congo hemorrhagic fever virus: progress in vaccine development. Diagnostics. 2023;13(16):2708.
16. Pınarlık F, Karaşahin Ö, Yanık A, Akça D, Sarıkaya Rİ, Güllü D, et al. Assessment of seroprevalence and neutralizing antibodies for healthcare worker protection in a Crimean-Congo hemorrhagic fever endemic area. International Journal of Infectious Diseases. 2026:108711.
17. S. Celina S, Černý J. Genetic background of adaptation of Crimean-Congo haemorrhagic fever virus to the different tick hosts. PLoS One. 2024;19(4):e0302224.